



Provided by the author(s) and University of Galway in accordance with publisher policies. Please cite the published version when available.

Title	Numerical modelling of pile foundation angular distortion
Author(s)	Sheil, Brian B.; McCabe, Bryan A.
Publication Date	2015-05-16
Publication Information	Sheil, Brian B., & McCabe, Bryan A. (2015). Numerical modelling of pile foundation angular distortion. <i>Soils and Foundations</i> , 55(3), 614-625. doi: http://dx.doi.org/10.1016/j.sandf.2015.04.012
Publisher	Elsevier
Link to publisher's version	http://dx.doi.org/10.1016/j.sandf.2015.04.012
Item record	http://hdl.handle.net/10379/6299
DOI	http://dx.doi.org/10.1016/j.sandf.2015.04.012

Downloaded 2024-04-24T14:17:59Z

Some rights reserved. For more information, please see the item record link above.



Cite as:

Sheil, B.B. and McCabe, B.A. (2015) Numerical modelling of pile foundation angular distortion, *Soils and Foundations*, Vol. 55, pp. 614-625.

DOI:10.1016/j.sandf.2015.04.012

Numerical modelling of pile foundation angular distortion

Brian B. Sheil

PhD Candidate, College of Engineering and Informatics, National University of Ireland, Galway.

Bryan A. McCabe

Lecturer, College of Engineering and Informatics, National University of Ireland, Galway, Ireland. Corresponding author, phone +353 (0) 91 492021, e-mail: bryan.mccabe@nuigalway.ie

Abstract

In this paper, the PLAXIS 3-D Foundation finite element (FE) software package, in conjunction with the nonlinear Hardening Soil (HS) constitutive model, is employed in an extensive parametric study of the angular distortion of piled foundations which has been documented as the most influential settlement characteristic in the cracking of buildings. Numerical results are appraised in the context of acceptable limits for angular distortion recommended in the literature and set out in geotechnical building codes since there is currently no guidance in the literature on appropriate pile cap rigidities to remain safely within these limits. Results from the parametric study were validated by comparing to measured differential settlement characteristics from buildings and full-scale pile groups documented in the literature with good agreement. In addition, the numerical data has been formulated into a set of fully-normalised trends; although a relatively wide range of variables are considered in the parametric study, a consistent trend between the average settlement performance and angular distortion for corresponding pile cap rigidities was evident. These trends present design engineers with a useful resource for estimating the angular distortion of piled foundations.

1. Introduction

The past couple of decades has seen a significant increase in the number of structures, particularly tall buildings, founded on piled foundations (Poulos 2001). In parallel, the focus of foundation design has shifted from ultimate limit state design to serviceability limit state design, and on the serviceability front, designers are increasingly considering differential settlements as well as maximum settlements in a foundation system. While maximum settlements of foundation systems have been received ample treatment in the literature, differential settlements have received less attention.

Where investigations of differential settlement have been reported, they relate to piled raft foundations in the main, e.g. Hirokoshi & Randolph (1998), Prakoso & Kulhawy (2001), Reul and Randolph (2004) and Cho *et al.* (2012). A number of these studies found that optimizing the design of a piled raft foundation involves locating piles near the centre of the foundation in order to minimise total differential settlements. In addition, parametric analyses identified the ratio of the pile group width to the pile raft width, group size, raft-soil stiffness ratio and the applied load configuration as having the greatest impact on differential settlements whereas pile length was deemed less influential.

While those studies considered the *magnitude* of differential settlements occurring across a piled raft, Skempton and MacDonald (1956) identified the radius of curvature as the most influential settlement characteristic causing cracking of buildings. They compiled a database of 98 case histories with the goal of developing limits for total and differential settlement of various foundations. Since the radius of curvature proved very difficult to measure accurately, they proposed angular distortion (β) as a more practical measure of differential settlement, defined as the ratio of the differential settlement to the horizontal distance between measurement stations.

A selection of the limits for β documented in the literature are presented in Table 1 through observations of damage to buildings founded on both clay and fill. The limits presented by Zhang and Ng (2005) were derived from a database of the settlement characteristics of 300 buildings within a probabilistic framework. In light of these studies, there now appears to be a general consensus in the literature that angular distortion greater than 1/300 is likely to induce damage in ordinary buildings, although Eurocode 7 has recently set out a more conservative 1/500 tolerable limit. Also relevant is Rethati's (1961) observation that 91% of the damage from his database was associated with buildings of two storeys or lower and concluded that

the rigidity of the supported structure should also be taken into account when considering angular distortion.

While the extent of angular distortion likely to cause building damage is now relatively well established, there remains a considerable lack of information in the literature on the rigidity of piled foundations required to comply with these limits. Moreover, in cases where angular distortion levels are relatively low, there is potential for considerable savings in foundation construction by optimizing the design of the pile cap, particularly for larger group sizes. In this paper, the PLAXIS 3-D Foundation finite element (FE) software package, in conjunction with the nonlinear Hardening Soil (HS) constitutive model, has been employed in an extensive parametric study of the angular distortion of piled foundations. Numerical results are appraised in the context of aforementioned limits for angular distortion. In addition, results from the parametric study are validated by comparing to measured differential settlement characteristics from buildings and full-scale pile groups documented in the literature. The numerical data is then formulated into fully-normalised trends which are intended to provide design engineers with a useful resource for estimating the angular distortion of piled foundations.

2. Details of the finite element modelling

2.1. Default HS parameters

The default HS soil parameters used in the parametric study are documented in Sheil and McCabe (2014). E_{oed} was determined from oedometer tests while E_{50} and E_{ur} were determined from triaxial compression test in primary loading and unloading/reloading, respectively. In addition, the parameter m was determined by curve-fitting to the stress-strain curve in triaxial compression. It has already been shown by Sheil and McCabe (2014) that these parameters represent the behavior of a soft clay/silt site at Belfast, Northern Ireland and predict the load-displacement behavior of a single pile and 5-pile group in this clay/silt (McCabe and Lehane 2006) very well. In addition, these parameters were used to arrive at a finite element-based empirical approach for the prediction of pile group settlement performance which compared well to a database of case histories in a range of clay types (Sheil and McCabe 2014). Obviously, the parametric study has necessitated variations upon some of the default parameters.

2.2. FE model parameters

The pile/soil parameters considered in the study are illustrated in Fig. 1. The default pile length (L) and diameter (D) are 6.0 m and 0.282m, respectively (the diameter gives an equivalent pile area to that of a square pile of width 0.25 m). These dimensions are based on pile sizes tested by McCabe and Lehane (2006). E_1 is the stiffness of the upper layer, E_2 is the stiffness of the lower layer, and the boundary between them occurs at a depth h below ground level, where h is greater than or equal to L . In all analyses, a value of $h/L = 3$ was maintained except in section 4.7 where $h/L=1$. The depth below ground level to the bottom mesh boundary, H , was chosen as $3L$ so that the lower mesh extremity had no effect on the FE output. Likewise, the lateral boundaries of the FE model for each analysis were located at a distance such that no influence was recorded on output.

Other features of the model are shown in Fig. 2 (the illustration is for a free-standing 16-pile group). 15-node wedge elements were used in the study comprising of 6-node triangular elements in the horizontal direction and 8-node quadrilateral elements in the vertical direction. Symmetry was exploited to reduce the number of elements used in the mesh. In all analyses, the mesh was refined in zones of high stresses near the piles. Coarse, medium and fine meshes were used to confirm mesh convergence for all analyses. Further details are available in Sheil and McCabe (2014).

2.3. Stages of analysis – free-standing groups

Although both piled rafts and free-standing pile groups are considered in this study, free-standing pile groups form the basis of the parametric study in section 4. Free-standing pile foundations have served as a common means for supporting offshore platforms and wind turbines in shallow water depths, for example (Gavin et al. 2011). The stages used in the analysis of a free-standing pile group are defined as follows:

- (i) Inclusion of interface elements in the soil model to allow for pile-soil slip.
- (ii) Initial stress generation by the K_0 procedure, a special calculation method available in PLAXIS.
- (iii) Installation of the concrete piles reflected by changing appropriate elements to a linear elastic material with a Young's Modulus of 30 GPa (in compression) and a Poisson's ratio, ν , of 0.15.
- (iv) Excavation of soil to a depth of 0.5 m below the pile heads. For a free-standing pile group in PLAXIS, it is necessary to excavate the soil below the pile cap so that it does

not come into contact with the ground surface. To ensure that the excavation of the soil in stage (iv) did not induce changes to the initial stresses in the soil, a dummy material was introduced to a height of 0.5m above the soil profile with weight density $\gamma=0 \text{ kN/m}^3$.

- (v) Installation of the pile cap (modelled as a ‘floor’ in PLAXIS) along the top of the pile group. Floors in PLAXIS are composed of 6-node triangular plate elements. Both the Young’s Modulus and thickness of the pile cap were varied in the parametric analyses presented later.
- (vi) Pile group loading by placing a compressive uniformly-distributed load on the top surface of the pile cap, as used by Cheung *et al.* (1988). Moreover, Reul and Randolph (2004) documented that a uniformly-distributed load is more likely to induce differential settlements of a piled raft than a loading system representative of loads transferred from exterior walls. However, in section 4.8 pile loading applied through the columns of the framed structure is also considered; the total loading was applied over n storeys as a UDL representing an average FS in keeping with the preceding analyses.

3. Basis for parametric study

3.1. Definition of pile cap flexibility

A goal of this study is to relate angular distortion to pile cap flexibility. Various analytical expressions that have been developed to describe the flexibility of a pile cap. The form of these expressions have their origin in plate bending theory, such as the expression given in Eq. (1) (Timoshenko and Woinowsky-Krieger 1959):

$$K_p = \frac{E_p t_p^3}{12(1-\nu_p^2)} \quad (1)$$

where K_p is the bending stiffness of a plate, E_p is the Young’s Modulus of the plate; t_p is the thickness of the plate and ν_p is the Poisson’s ratio of the plate.

Brown (1975) provided a more appropriate expression for the rigidity of a raft by incorporating the influence of the interaction between the raft and underlying soil defined as follows:

$$K_r = \frac{4E_r B_r t_r^3 (1-\nu_s^2)}{3\pi E_s L_r^4} \quad (2)$$

where K_r is the relative raft-soil stiffness; E_r is the Young's modulus of the raft; B_r is the width of the raft; L_r is the length of the raft; t_r is the thickness of the raft; ν_s is the Poisson's ratio of the soil and E_s is the Young's Modulus of the soil.

These approaches, however, do not take into account the influence of the piles on the rigidity of the pile cap. The definition of pile cap flexibility by Cheung *et al.* (1988), shown in Eq. (3) has been adopted in the present study:

$$K_r = \frac{E_c t_c^3}{12(1-\nu_c^2)} \frac{w_s}{s^2 P_{ave}} \quad (3)$$

where E_c is the Young's modulus of the cap; t_c is the thickness of the cap; ν_c is the Poisson's ratio of the cap; w_s is the settlement of a single pile under the same average load; s is the pile-to-pile spacing and P_{ave} is the average load per pile in the group. Cheung *et al.* (1988) reported that, in general, pile caps are designed with $\log K_r > 1$. However, values of $\log K_r$ of a number of well-documented pile foundation case histories have been computed by the authors and were found to lie between -1.5 (Thorburn *et al.* 1983) and 1.5 (McCabe and Lehane 2006). In light of this, a relatively broad spectrum of K_r values has been considered in the present study i.e. $|\log K_r| \leq 4$, although caps with $|\log K_r| \leq 2$ are of primary interest.

3.2. Overview of parametric study

Angular distortion is defined as follows:

$$\beta = \frac{\delta}{l} \quad (4)$$

where δ is the differential settlement and l is the horizontal distance between 'measuring stations' which were chosen by Skempton and MacDonald (1956) as the locations of the footings supporting the building (see Fig. 3). It can also be seen from Fig. 3 that Δ denotes the maximum *differential* settlement of the footing (in this case between stations c and e) ρ_{max} denotes the maximum settlement of the foundation (in this case station e experiences the greatest settlement). Therefore the locations of the pile heads were used as the 'measuring stations' in this study.

In general, the value of β is very small and for convenience, the inverse of β (i.e. β^{-1}) is plotted in the subsequent sections which can be considered as a form of 'angular rigidity'. The values of β^{-1} presented subsequently correspond to the minimum values for each (square)

group unless specified otherwise; these occurred between the corner pile and next inner pile along the diagonal in almost all cases.

In general, a factor of safety (FS) of 1.35 on the capacity of a single pile was used as the basis of the parametric study representing the FS on unfavourable permanent loads recommended by Eurocode 7. The capacity of a single pile was defined as the load required to generate a pile head displacement of $0.1D$ in this study where D is the pile diameter. The influence of load level has also been considered in section 4.2.

The piles in the group have been labelled alphabetically starting from the centre pile of each group moving outwards as shown in Fig. 4 for a 9-pile group; thus pile a is the centre pile for each group while pile c , pile f , pile j , and pile o are the corner piles for group sizes of 3^2 , 5^2 , 7^2 and 9^2 (the limiting size for this study), respectively. Also shown on Fig. 4 is the geometry of the pile cap where B is the shortest distance between the edge of the cap and the centre of the outer piles.

3.3. Comparison to linear elastic analyses

As an initial validation exercise, PLAXIS output using a linear elastic (LE) soil model has first been compared to analytical predictions also based on LE theory (Cheung *et al.* 1988). A two-layered profile having constant soil stiffness with depth (see Guo *et al.* (1987) for full details) is the basis of the predictions in Figs. 5 and 6. The pile-soil properties adopted in the present analyses in Figs. 5-6 were thus chosen to correspond to the properties adopted by those authors. In Fig. 5, the variation in P_a/P_{ave} and P_c/P_{ave} has been plotted versus $\log K_r$ where P_a is the load corresponding to pile a (see Fig. 4), P_c is the load corresponding to pile c and P_{ave} is the average load per pile in the group. It can be seen that results using the LE soil model in PLAXIS agree reasonably well with the LE predictions documented by Cheung *et al.* (1988). While both approaches are based on LE theory, the method by Cheung *et al.* (1988) does not consider the cap-pile-soil continuum directly which contributes to some of the differences in the curves. Present predictions support the findings of Cheung *et al.* (1988) that pile groups with a flexible pile cap ($\log K_r \leq -2$) do not necessarily impose equal load on all piles.

In Fig. 6, normalised differential settlement, Δ_{xy}/w_s , has been plotted versus $\log K_r$ for the same analyses where Δ_{xy} is the differential settlement between pile x and pile y in the group. It can again be seen that results using the LE soil model in PLAXIS agree well with results by

Cheung *et al.* (1988). It is also notable, however, that the method of interaction factors can significantly under-estimate the differential settlement of flexible pile groups due to the assumption of equivalent pile head loads. Interestingly, the predictions for flexible pile group settlement documented by Poulos (1968) may still provide a suitable upper-bound estimate for higher pile cap rigidities ($\log K_r \geq 0$).

3.4. Adopted pile cap conditions

As mentioned, the majority of studies that have investigated the differential settlement of piled foundations have considered piled rafts whereas the contribution provided by cap-soil interaction has received much less attention. In Fig. 7, the variation of β^{-1} of a free-standing group has been compared to a similar group where the cap is in contact with the soil surface (i.e. a piled raft). Similar stages were used for the analysis of a piled raft as those set out in section 2.3, although the dummy layer was not required and was thus not included in the model; all other model parameters were similar. In addition, the same average load per pile was applied to the piled raft as was applied to the free-standing group (i.e. FS=1.35 on single pile capacity).

From Fig. 7, cap-soil interaction surprisingly has little influence on the value of β^{-1} required by Eurocode 7 for a value of $B/s=0$. It can be seen that increasing the value of B/s from 0 to 0.5 has a significant influence on β^{-1} where the curves for the two foundation types diverge significantly. From these findings, it is clear that a value of $B/s=0.5$ is more appropriate for maintaining acceptable values of β^{-1} , particularly for free-standing pile groups. Since there is little guidance in the literature on commonly-employed cap over-hang distances, the authors adopt a free-standing pile group in conjunction with a value of $B/s=0$ henceforth in order to err on the side of conservatism; this is also in keeping with the modelling of Cheung *et al.* (1988).

3.5. Influence of adopted soil profile

Due to the uncertainty inherent in the selection of OCR for sandy soils, the OCR of the silty sand (see Sheil and McCabe 2014) has been varied from a value of 1 to 4 in Fig. 8. It can be seen that for the adopted profile, the assumed values of OCR has a negligible influence on PLAXIS output, largely due to the relatively small layer thickness.

In addition, as a check that the findings of the present study are not unique to the particular soil properties adopted, results determined using a completely different soil profile have been presented in Fig. 9. The analyses are based upon the HS parameters of the well-documented Boston Blue Clay (BBC; see McCabe and Sheil 2014) and have been compared to previous results using parameters based on the Belfast site. It is clear that while soil type has a minor influence on β^{-1} , the difference is consistent over the spectrum of K_r values considered.

4. Parametric study

4.1. Influence of constitutive model

The influence of the stress-dependency of soil stiffness has been investigated in Fig. 10 in which results using the HS model in PLAXIS have been compared to results determined using a LE soil model with a constant vertical stiffness profile. The properties used for the HS model here and henceforth in the paper are those documented in Sheil and McCabe (2014). The properties of the LE soil model were chosen based on the equivalent small-strain stiffness values of the HS properties calibrated using the initial stiffness of the single pile load-displacement response (more details also given in Sheil and McCabe 2014).

In Fig. 10, β^{-1} has been plotted against $\log K_r$ using both soil models. The minimum value of β^{-1} was calculated between the corner pile and next inner pile (i.e. pile *c* and pile *a*, respectively, for a group with $N=9$). It is clear that the consideration of soil nonlinearity has a significant influence on β^{-1} . A number of studies have testified to the validity of LE analysis in pile group design and load test interpretation in appropriate situations such as displacement interaction between adjacent piles, e.g. Mandolini *et al.* (2005), Leung *et al.* (2010). However, this study shows that LE analyses provide unconservative predictions of β^{-1} .

4.2. Influence of load level

In Fig. 11a, the influence of load level on β^{-1} has been investigated where results using a FS of 2.5, representing a more traditional FS for pile groups (Sheil and McCabe 2014) have been compared to the nonlinear results presented in the previous section (where a value of FS=1.35 was used). In order to remain within acceptable limits set out by Eurocode 7, values of $\log K_r$ of approx. -1 and 0 are required for a FS of 2.5 and 1.35, respectively. For the purpose of examining the contribution of soil nonlinearity to these differences, load-transfer curves are plotted in Fig. 11b at depths within the fill, silty sand and sleetch layers. It can be seen that for a FOS=1.35, significant nonlinearity is evident in the load-transfer response. It is therefore

obvious that an underestimation of the load level experienced by a piled foundation also leads to non-conservative predictions of β^{-1} .

4.3. Influence of N

To investigate the effect of increasing the size of the group, N , predictions determined for 3^2 , 5^2 and 9^2 groups have been compared in this section. Intuitively, the increase in N causes a reduction in β^{-1} as shown in Fig. 12; the required values of $\log K_r$ to remain within the acceptable limits set out in the Eurocodes for a 3^2 pile and 9^2 pile group are significantly different.

In addition, a cross-section through the groups (see Fig. 13) was taken to investigate the distribution of β^{-1} throughout the three group sizes. In Fig. 14, an example of the distribution of β^{-1} have been plotted against the location (i.e. pile a through pile o) within the group for a value of $\log K_r$ equal to 2. The distribution confirms that the minimum values of β^{-1} occurred between the corner and next inner pile for each group size.

4.4. Influence of s/D

The influence of the pile spacing-to-diameter (s/D) on the settlement performance of piled foundations has been widely investigated in the literature; its influence on β^{-1} is investigated in Fig. 15 by varying the value of s/D from 2 to 5 for a 9-pile group. It is clear that a reduction in s/D has an adverse effect on β^{-1} , to the point where the corresponding values of $\log K_r$ needed for compliance with the Eurocode limit differ by almost an order of magnitude. In addition, the authors have verified that there is a unique solution for a particular value of s/D , i.e. similar results for β^{-1} were observed for a group with $D=0.3\text{m}$ ($s=0.9\text{m}$) and $D=0.6\text{m}$ ($s=1.8\text{m}$).

4.5. Influence of group configuration

The influence of group geometry has also been taken into account where the value of m/n has been varied between 1 and 9 where m and n are defined in Fig. 16. The location of the minimum values of β^{-1} for the different group configurations was not obvious when $m \neq n$ and thus pile cap deformation contours were used for this purpose. Fig. 17 depicts the contours

for a cap with $m/n=2$ (quarter-symmetry); it can be seen that the contours become closer near the corner of the pile cap indicating the location of the minimum value of β^{-1} .

From Fig. 18, surprisingly an increase in the value of m/n does not have an influence on the required cap rigidity recommended by Eurocode 7. Square groups (i.e. $m/n=1$) appear to exhibit a broader range of angular rigidities while oblong configurations reach lower maximum values of β^{-1} with increasing m/n .

4.6. Influence of L/D

The influence of pile slenderness was investigated by varying the diameter of the piles while maintaining a value of $s/D=3$. In Fig. 19, the variation in β^{-1} has been plotted for values of L/D equal to 20 and 50. In the course of this study, it was verified that the bending moments induced by the axial loads are smaller than the yield moment, M , of the pile calculated as:

$$M = f_p \cdot z \quad (5)$$

where f_p is the yield stress of the pile material (conservatively chosen as 30 MPa i.e. mass concrete) and z is the elastic section modulus. In comparison to the influence of the parameters considered previously, it can be seen that the increase in L/D corresponds to a marginal reduction in β^{-1} .

4.7. Influence of E_2/E_1

For the purpose of investigating the influence of varying E_2/E_1 , a stiff bearing stratum has been included in the soil model where a value of $h/L=1$ was adopted. The soil properties of the stiff bearing stratum are identical to those adopted for the soft clay except that the soil stiffness parameters have been multiplied by a factor of E_2/E_1 similar to a previous study conducted by the authors (McCabe and Sheil 2014). Fig. 20a and 20b presents the results of these analyses for values of E_2/E_1 ranging from a value of 1 to 30 for $N=9$ and $N=81$, respectively. As expected, an increase in the stiffness of the bearing stratum at the base of the piles increases the angular rigidity of the group; to the point where both group sizes founded on a stratum with $E_2/E_1=30$ have angular rigidity that is acceptable according to Eurocode 7 regardless of the stiffness of the pile cap although it is recognised that this is also dependant on the adopted value of L/D . From these results, it is clear that piled foundations founded on stiffer stratum have significant scope for refining the design of the pile caps.

4.8. Influence of the supported superstructure

Rethati (1961) noted that the influence of the rigidity of the supported superstructure should be taken into account when considering the angular distortion of a piled foundation. However, Grant *et al.* (1974) documented little influence of the number of storeys and width of a building on the ratio of maximum angular distortion to the maximum settlement of the building.

In the most generalized form, the supported superstructure may be idealized as a three-dimensional frame similar to that employed in a number of soil-foundation-structure studies reported in the literature, e.g. Cai *et al.* (2000) and Dutta & Roy (2002) (see Fig. 21). The framed structure is composed of three-noded line (beam) elements. The cross-sectional dimensions of the beams and girders were arbitrarily chosen as 0.3m x 0.3m respectively with a (concrete) Young's modulus of 30 GPa. The height of the columns was chosen as 2.5m representing a typical height of 1 storey where n is the number of storeys. An illustration of the frame in the model is provided in Fig. 21 for an $N=9$ group.

Fig. 22 presents the results of the variation in β^{-1} with $\log K_r$ for n ranging between 0 and 5. The additional rigidity of the superstructure improves the angular rigidity of the group which supports the findings of Rethati (1961). It is clear that the additional rigidity provided by the supported superstructure should be taken into account for further optimization of the pile cap design. It is noticeable, however, that the effect of n on β^{-1} decreases with increasing n over the range of interest i.e. $|\log K_r| \leq 2$.

4.9. Group optimization

A common feature of the aforementioned studies on the differential settlement of piled rafts was the consideration of the 'optimized' design. These optimized designs were aimed at reducing differential settlement but did not consider angular distortion/rigidity. The parametric analyses presented herein identified a number of variables that have the effect of increasing angular rigidity. Table 2 presents the parameters, and their respective ranges, considered in the previous parametric analyses. In addition, the authors have also attempted to summarise the relative influence of each pile/soil parameter on β^{-1} by documenting their effect on the value of $\log K_r$ corresponding to the Eurocode limit (EC7), which is of most

interest. The authors have used an “arrow” system for this purpose although it is recognised the influence of each parameter depends on the ranges that were arbitrarily chosen.

For a pre-determined building footprint, it is clear that it is more advantageous to use longer piles with fewer pile numbers; reducing the number of piles benefits angular rigidity two-fold in that the pile-to-pile spacing may also then be increased. The study also identified the effectiveness of founding a pile group on a stiff stratum. If these are not sufficient (or feasible), the authors have investigated the effect of reducing the length of the outer perimeter of piles since the lowest values of β^{-1} occurred near the corner pile in most cases. This is shown in Fig. 23 where L_o is the length of the outer perimeter of piles. The distribution of β^{-1} for a standard group (i.e. $L_o/L=1$) has been compared to that within an optimized group with a values of L_o/L between 0.5 and 0.75 in Fig. 24 where the value of $\log K_r=0$ was chosen arbitrarily. The load applied to the optimized groups was adjusted in order to maintain the same average FS per pile within the group. It is clear that reducing the lengths of piles in the outer ring is also effective in increasing β^{-1} within the groups.

5. Comparison to measured data

5.1. Databases

For the purpose of putting some practical context on predictions of differential group settlement using the present model, PLAXIS results presented previously have been compared to three databases documented in the literature. The databases compiled by Skempton and MacDonald (1956), and later extended with additional information by Grant *et al.* (1974), documented measured settlement characteristics of buildings. Those databases consisted of both isolated footings and rafts in clay; data in sand has also been included by way of comparison. The third database considered was that compiled by Mandolini (2005) of the settlement characteristics of a number of large-scale pile foundation case histories. Those foundations ranged in size from 4-pile to as large as 6,000-pile groups. The PLAXIS data presented in this section is derived from the parametric studies in the preceding sections. Table 2 documents the range of variables present in the PLAXIS data used in the following sections.

5.2. Maximum differential settlement

Maximum differential settlements have been the subject of a number of numerical studies (associated with piled rafts) and have also featured in all three of the aforementioned databases. In Fig. 25, PLAXIS results have been compared to measured field data where the average settlement of the foundation, ρ_{ave} , is plotted against the maximum differential settlement of the foundation, Δ_{max} . In this study, ρ_{ave} is calculated according to Reul and Randolph (2004) as:

$$\rho_{ave} = (2\rho_{centre} + \rho_{corner})/3 \quad (5)$$

where ρ_{centre} and ρ_{corner} are the settlements at the centre and corner of the pile cap, respectively. In general, output from PLAXIS appears to agree well with the measured data presented in the figure. Moreover, there appears to be a relatively linear trend in the relationship between the two measures of settlement.

5.3. Angular distortion

Grant *et al.* (1974) presented a relationship between ρ_{ave} and β which has been compared to PLAXIS data in Fig. 26. Both the numerical and measured data show similar trends and reasonable agreement is evident. The authors attribute the lack of exactness in the agreement between measured and numerical data to:

- The measure for overall foundation settlement (ρ_{ave}) which is not normalised and is thus influenced by a range of pile/soil parameters and
- The conservatism inherent in the numerical data arising from the parameters that formed the basis of the parametric study discussed in section 3.

6. Fully normalised trends from numerical results

The authors have extended the results presented in the previous case to the case of fully normalised trends (i.e. η_{ave} versus β^{-1}) since η and β^{-1} are superior measures of pile foundation settlement performance.

In Fig. 27, the variation of β^{-1} with η_{ave} determined using PLAXIS output has been plotted for a range of values of $\log K_r$ for Belfast clay with $B/s=0$ and a FS=1.35. Therefore only variation in geometric parameters was considered in these plots, allowing a like-with-like

comparison. Best fit lines through the data have also been superimposed on the figure for each values of $\log K_r$, where $\log K_r \leq 0$ data have been combined because they showed good agreement. The limit set out in Eurocode 7 has also been superimposed on the figure. It can be seen that a value of at least $\log K_r = 0$ is required to maintain the level of angular rigidity above the Eurocode limit. The findings presented in Fig. 27, which include the results with a variation in n from 0 to 5, support the study by Grant *et al.* (1974) who documented that the number of storeys had an insignificant influence on relationships between angular distortion and settlement performance. Values of R^2 of 0.88 for $\log K_r \leq 0$ indicates strong evidence of a relationship between foundation stiffness efficiency and angular rigidity.

In order to obtain an estimate of β^{-1} for a pile group foundation, the trends presented in Fig. 27 can be used in conjunction with an approach capable of obtaining an estimate of η_{ave} for the group. The simplified finite element-based approach documented by Sheil and McCabe (2014), which was developed using a similar framework to the present study, is a compatible way to estimate η_{ave} .

7. Conclusions

A numerical study of angular rigidity has been presented in this paper using the Hardening Soil model in the PLAXIS 3-D Foundation finite element software package. A number of consistent trends featured in the study thus allowing the following conclusions to be drawn.

- (a) The majority of studies on the subject of differential pile foundation settlement to date have considered overall differential settlements. Reports on damage to buildings, however, have identified angular distortion, β , as the most influential settlement characteristic in the serviceability of the supported superstructures.
- (b) A number of studies have attempted to reinforce the continued use of LE analyses in appropriate situations such as ‘interactive’ pile displacements. However, this study shows that stress-dependent soil stiffness has an important influence on predictions of angular rigidity, β^{-1} , when the group is modelled as a continuum; LE analyses provide unconservative predictions.
- (c) A parametric study was undertaken where a number of pile/soil parameters were varied in order to identify their relative influences on β^{-1} . The influence of the respective variables were qualitatively summarised by the authors following the parametric analyses.

- (d) Pile foundations may be optimised for angular rigidity where reducing the length of the outer perimeter of piles was shown to be very effective in increasing the distribution of angular rigidity within the group.
- (e) Obvious trends between group settlement performance (i.e. average stiffness efficiency) and angular rigidity were documented thus providing design engineers with a practical resource for the estimation of pile foundation angular distortion.

Acknowledgements

The first author is grateful for the support of the College of Engineering and Informatics Fellowship awarded by the National University of Ireland, Galway.

References

- Brown, P. T. "The significance of structure-foundation interaction." *Proc., Proceedings of the 2nd Australia-New Zealand Conference on Geomechanics*, IEQust.
- Cheung, Y. K., Tham, L. G., and Guo, D. J. (1988). "Analysis of pile group by infinite layer method." *Geotechnique*, 38(3), 415-431.
- Cho, J., Lee, J. H., Jeong, S., and Lee, J. (2012). "The settlement behaviour of piled raft in clay soils." *Ocean Engineering*, 53, 153-163.
- Gavin, K. G., Igoe, D., and Doherty, P. (2011). "Use of open-ended piles to support offshore wind turbines: a state of the art review." *Proceedings of the ICE - Geotechnical Engineering*, 164(GE4), 245-256.
- Grant, R., Christian, J. T., and Vanmarcke, E. H. (1974). "Differential settlement of buildings." *J. Geotech. Geoenviron. Eng.*, 100(9), 973-991.
- Guo, D. J., Tham, L. G., and Cheung, Y. K. (1987). "Infinite layer for the analysis of a single pile." *Computers and Geotechnics*, 3(4), 229-249.
- Horikoshi, K., and Randolph, M. F. (1998). "A contribution to the optimum design of piled rafts." *Geotechnique*, 48(2), 301-317.
- Jappeli "Settlement studies of some structures in Europe." *Proc., Proceedings 6th International Conference on Soil Mechanics and Foundation Engineering*, 88-92.
- Leung, Y. F., Soga, K., Lehane, B. M., and Klar, A. (2010). "Role of linear elasticity in pile group analysis and load test interpretation." *J. Geotech. Geoenviron. Eng.*, 136(12), 1686-1694.
- Mandolini, A., Russo, G., and Viggiani, C. (2005). "Pile foundations: Experimental investigations, analysis and design." *Ground. Eng.*, 38(9), 34-35.
- McCabe, B. A., and Lehane, B. M. (2006). "Behavior of axially loaded pile groups driven in clayey silt." *Journal of Geotechnical and Geoenvironmental Engineering, ASCE*, 132(3), 401-410.
- McCabe, B. A., and Sheil, B. B. (2014). "Pile group settlement estimation: suitability of nonlinear interaction factors." *ASCE Int. J. Geomech.*, In press. DOI:10.1061/(ASCE)GM.1943-5622.0000395.
- Poulos, H. G. (2001). "Piled-raft foundation: design and applications." *Geotechnique*, 127(1), 17-24.
- Prakoso, W. A., and Kulhawy, F. H. (2001). "Contribution to piled raft foundation design." *Journal of Geotechnical and Geoenvironmental Engineering*, 127(1), 17-24.
- Rethati "Behaviour of building foundations on embankments." *Proc., Proceedings of 5th International Conference on Soil Mechanics and Foundation Engineering*, 781.
- Reul, O., and Randolph, M. F. (2004). "Design strategies for piled rafts subjected to nonuniform vertical loading." *Journal of Geotechnical and Geoenvironmental Engineering*, 130(1), 1-13.
- Sheil, B. B., and McCabe, B. A. (2014). "A finite element based approach for predictions of rigid pile group stiffness efficiency in clays." *ACTA Geotechnica*, 9, 469-484.
- Skempton, A. W., and MacDonald, D. H. (1956). "The allowable settlement of buildings." *ICE Proceedings*, 5(Part III), 727-784.
- Thorburn, S., Laird, C., and Randolph, M. F. "Storage tanks founded on soft soils reinforced with driven piles." *Proc., Proceedings of the Conference of Recent Advances in Piling and Ground Treatment for Foundations*, ICE, 157-164.

- Timoshenko, S., and Woinowsky-Krieger, S. (1959). *Theory of plates and shells*, McGraw-Hill, New York.
- Wahls, H. E. (1994). "Tolerable deformations." *Geotechnical Special Publication No. 40*, ASCE, New York, 1611-1628.
- Zhang, L. M., and Y., N. A. M. (2005). "Probabilistic limiting tolerable displacements for serviceability limit state design of foundations." *Géotechnique*, 55(2), 151-161.

Table 1 Limits for angular distortion

Reference	Limits
Skempton & MacDonald (1956) Rethati (1961) Jappeli (1965)	$\beta < 1/300$
Wahls (1994)	$\beta < 1/125$ to $1/250$
Zhang & Ng (2005)	$\beta < 1/86 \pm 1/70$ (<i>intolerable</i>) $\beta < 1/357 \pm 1/417$ (<i>tolerable</i>)
Eurocode 7	$\beta < 1/500$

Table 2 Summary of parametric study

Pile/soil parameter	Min	Max	Influence on EC7 β^{-1}
Constitutive model	<i>LE</i>	<i>Nonlinear</i>	↑↑↑
Cap-soil interaction	<i>No</i>	<i>Yes</i>	↑
<i>B/s</i>	<i>0</i>	<i>0.5</i>	↑↑↑
Soil type	<i>Belfast</i>	<i>BBC</i>	↑
<i>FS</i>	<i>2.35</i>	<i>1.35</i>	↑↑
<i>N</i>	<i>3²</i>	<i>9²</i>	↑↑↑
<i>s/D</i>	<i>2</i>	<i>5</i>	↑↑
<i>m/n</i>	<i>1</i>	<i>9</i>	↑
<i>L/D</i>	<i>20</i>	<i>50</i>	↑
<i>E₂/E₁</i>	<i>1</i>	<i>30</i>	↑↑↑
<i>n</i> (height)	<i>0 (0)</i>	<i>5 (12.5 m)</i>	↑↑↑

↑: $\Delta \log K_r < 0.5$, ↑↑: $0.5 < \Delta \log K_r < 1$, ↑↑↑: $\Delta \log K_r > 1$

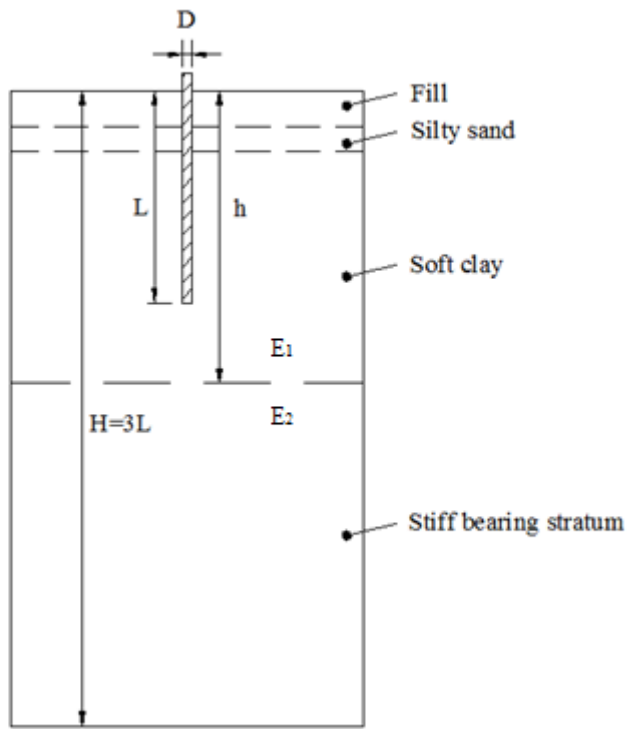


Fig. 1 Illustration of pile/soil parameters

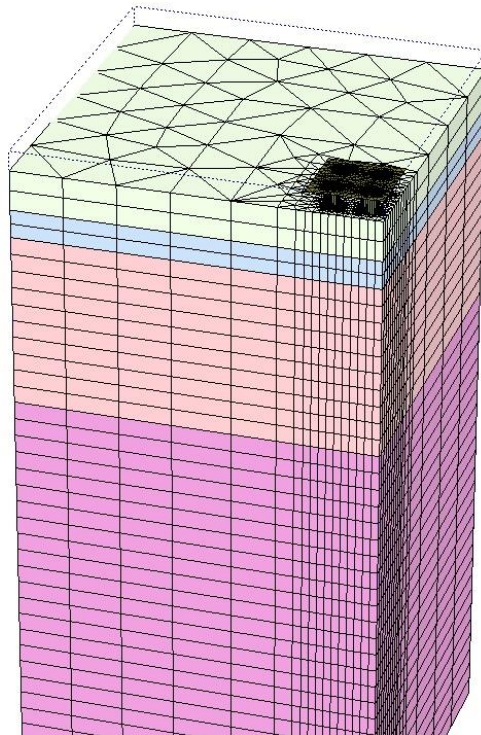


Fig. 2 Finite element mesh for free-standing 16-pile group

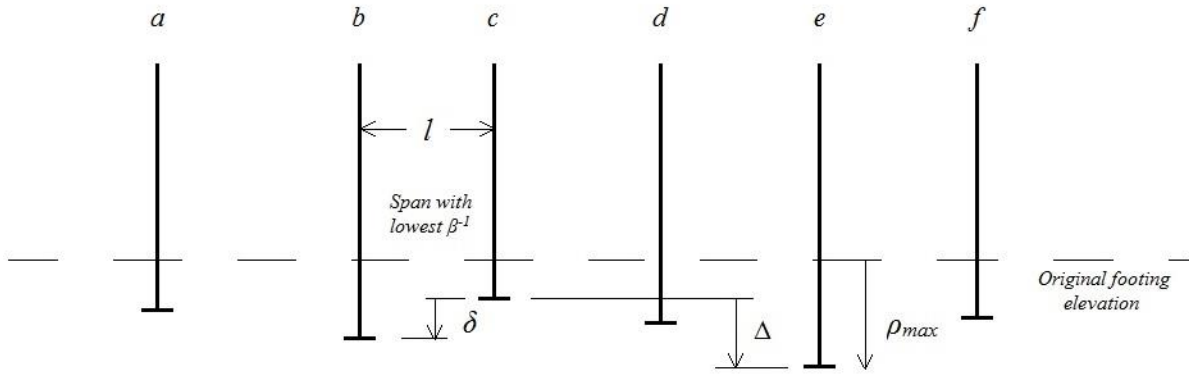


Fig. 3 Definition of settlement characteristics (adapted from Skempton and MacDonald 1956)

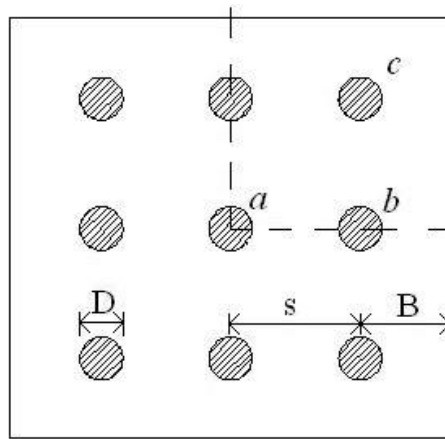


Fig. 4 Pile group geometry and labels for a 9-pile group

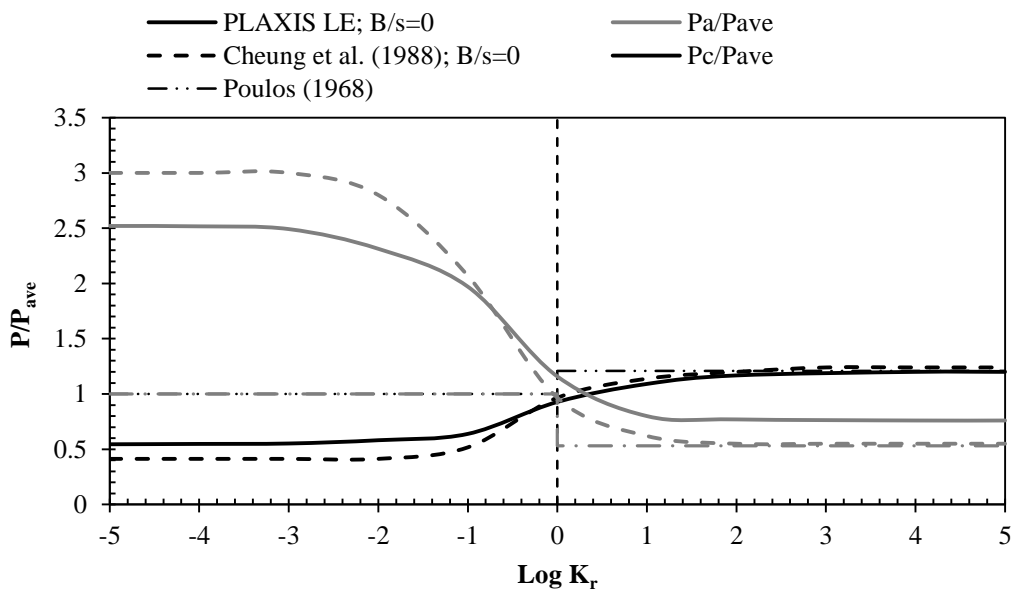


Fig. 5 Comparison of pile *a* and pile *c* load sharing to existing LE predictions; $s/D=3$, $N=9$

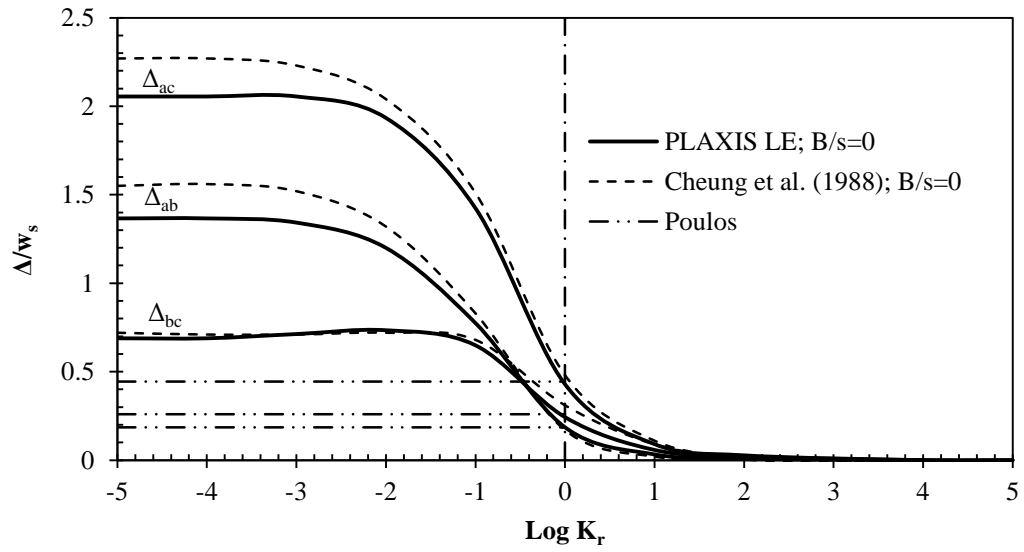


Fig. 6 Comparison of normalised differential settlement predictions; $s/D=3$, $N=9$

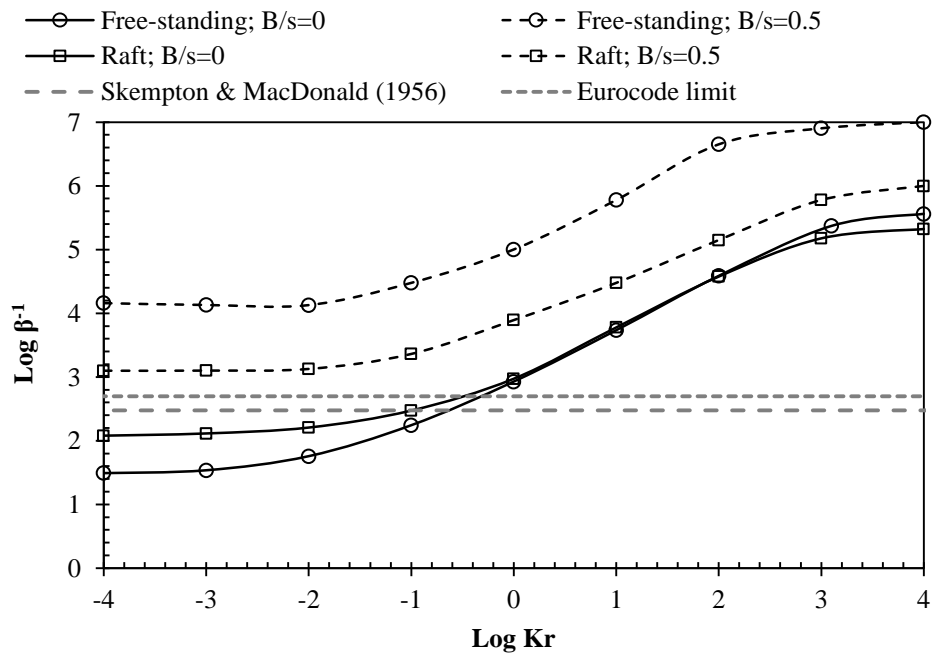


Fig. 7 Influence of cap-soil interaction & cap geometry on β^{-1}

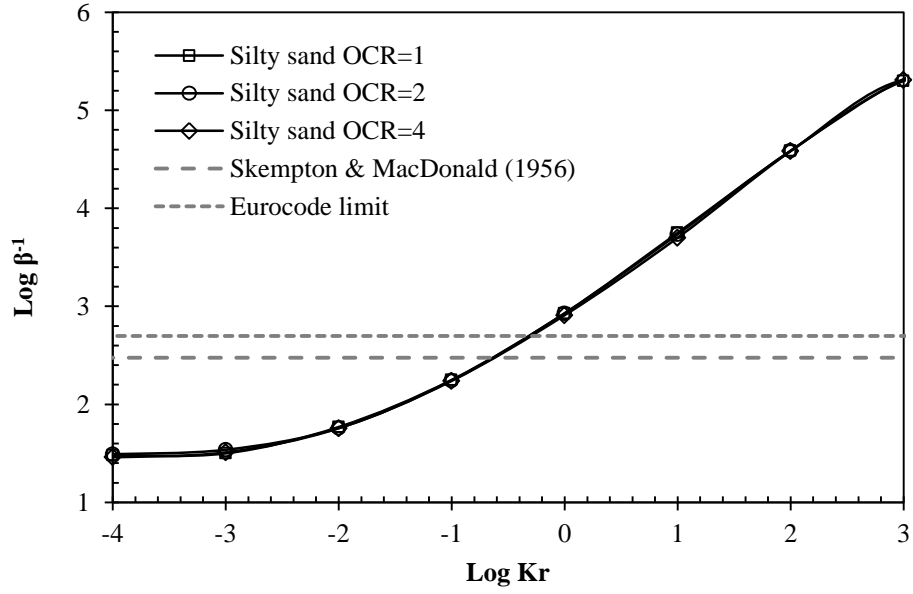


Fig. 8 Influence of silty sand OCR on β^{-1} ; $N=9$, $s/D=3$

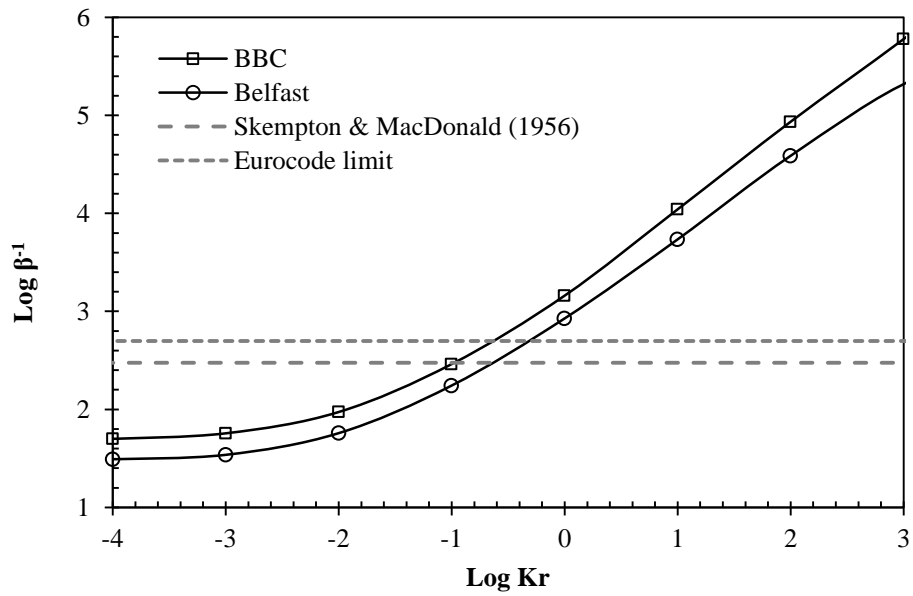


Fig. 9 Influence of soil profile on β^{-1} ; $N=9$, $s/D=3$

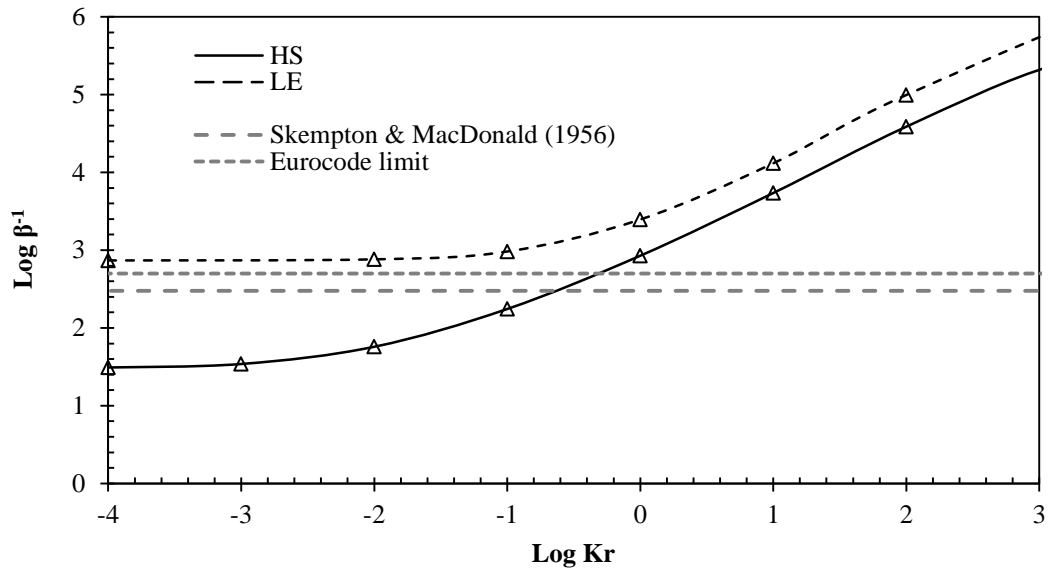


Fig. 10 Influence of soil nonlinearity on β^{-1} ; $N=9$, $s/D=3$

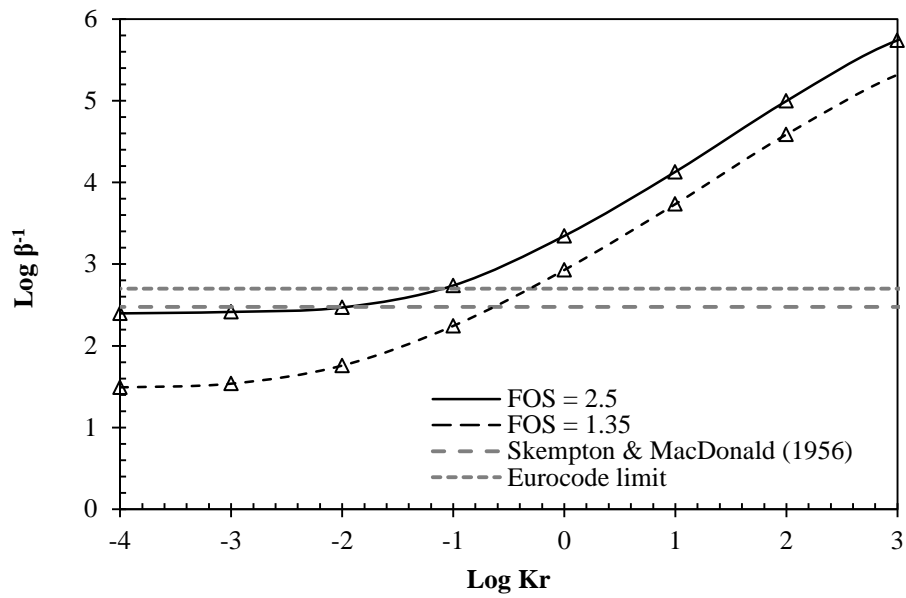


Fig. 11a Influence of load level on β^{-1} ; $N=9$, $s/D=3$

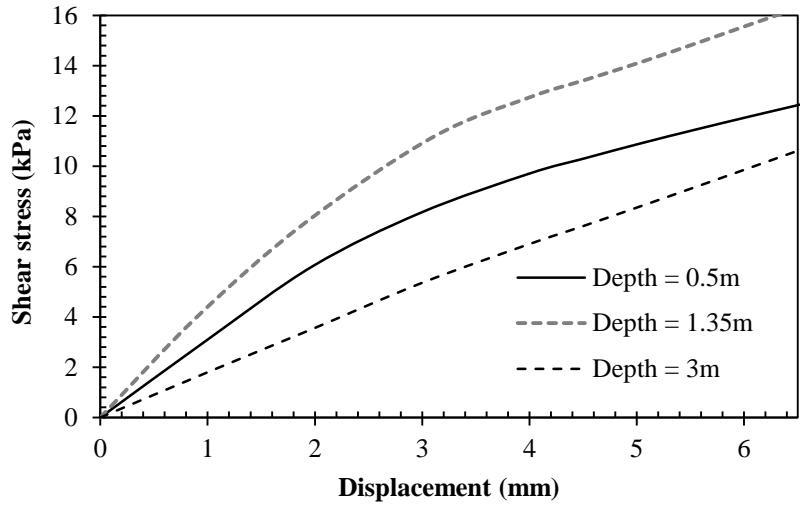


Fig. 11b Load-transfer curves for centre pile with FOS=1.35; $\text{Log}K_r=0$, $N=9$, $s/D=3$

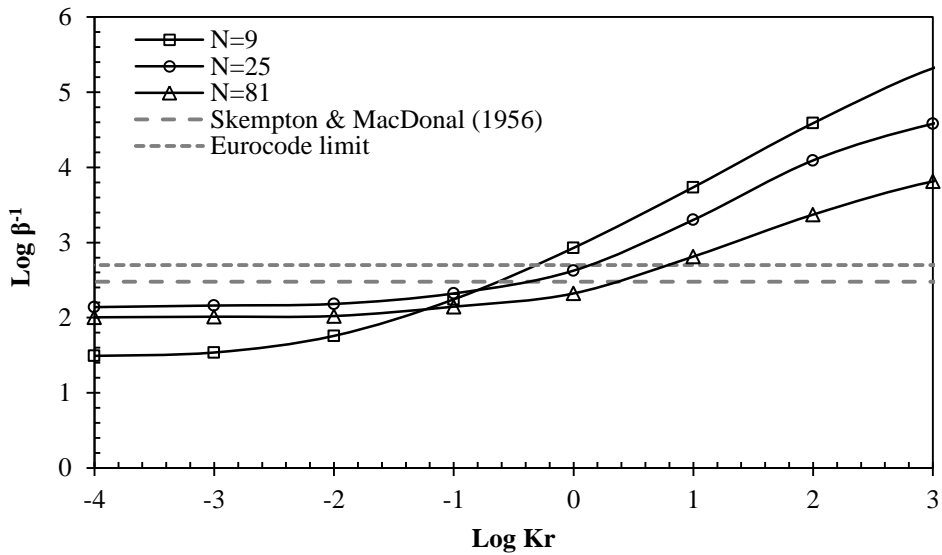


Fig. 12 Influence of group size on β^{-1} ; $s/D=3$

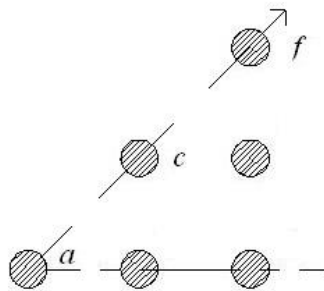


Fig. 13 Direction of cross-section taken through groups

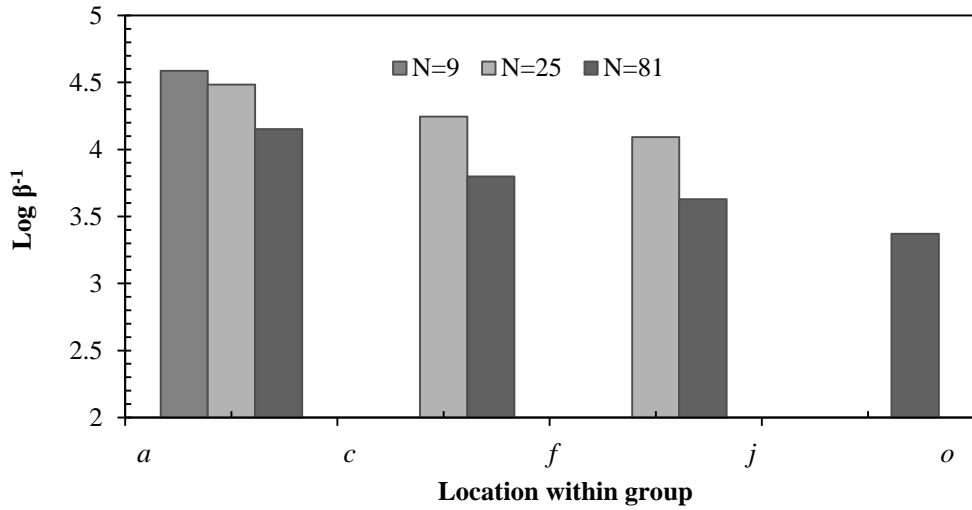


Fig. 14 Distribution of β^{-1} for $\text{log } K_r = 2$

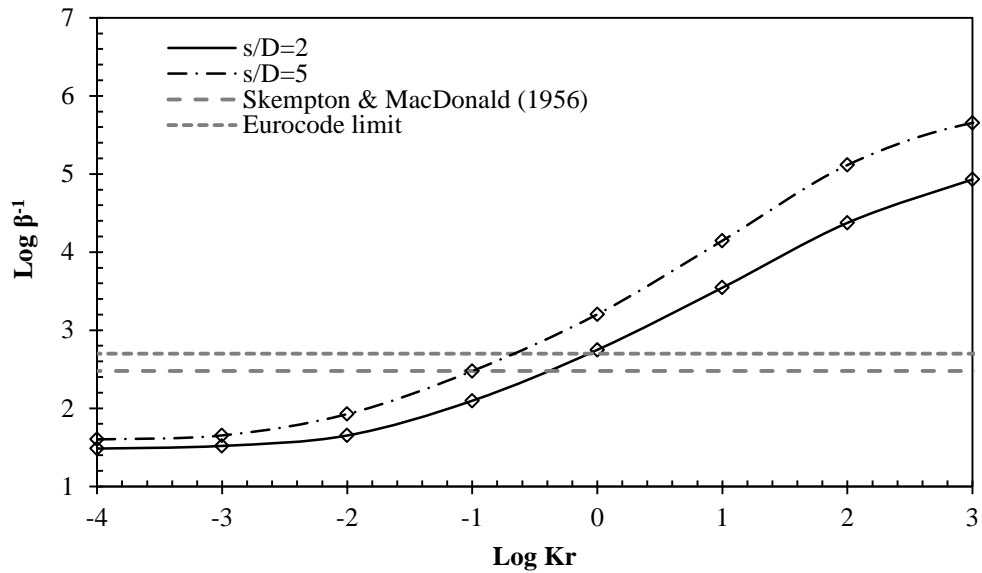


Fig. 15 Influence of s/D on β^{-1} for $N=9$

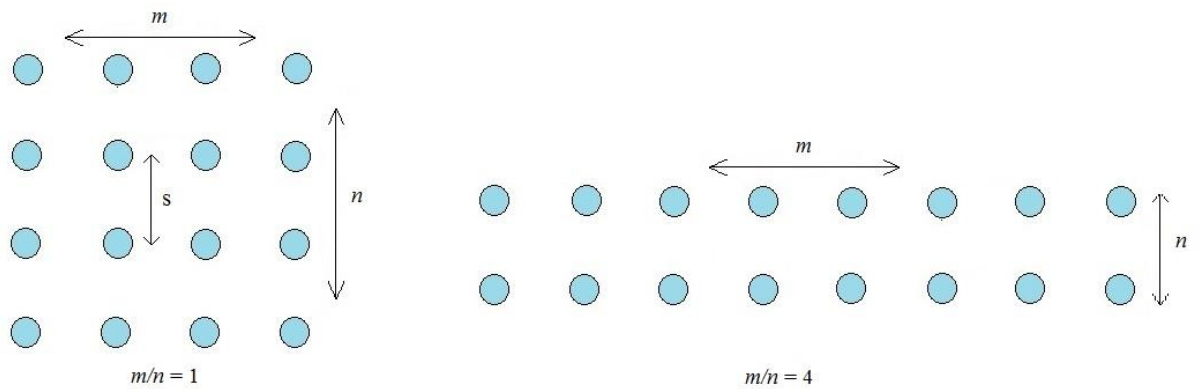


Fig. 16 Definition of m/n

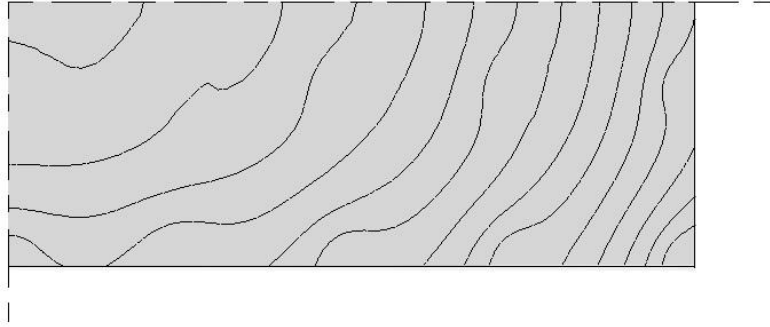


Fig. 17 Pile cap deformation contours; $\log K_r=0$, $m/n=2$, $N=36$

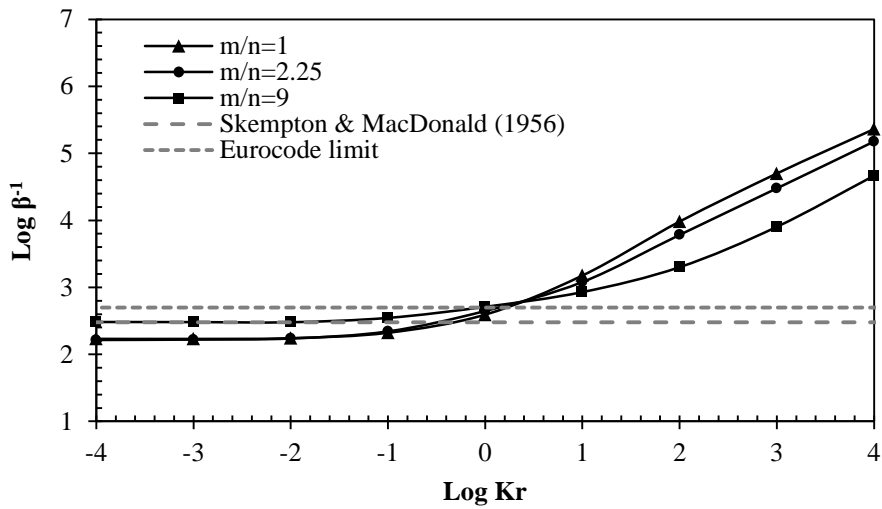


Fig. 18 Influence of group configuration on β^{-1} ; $N=36$, $s/D=3$

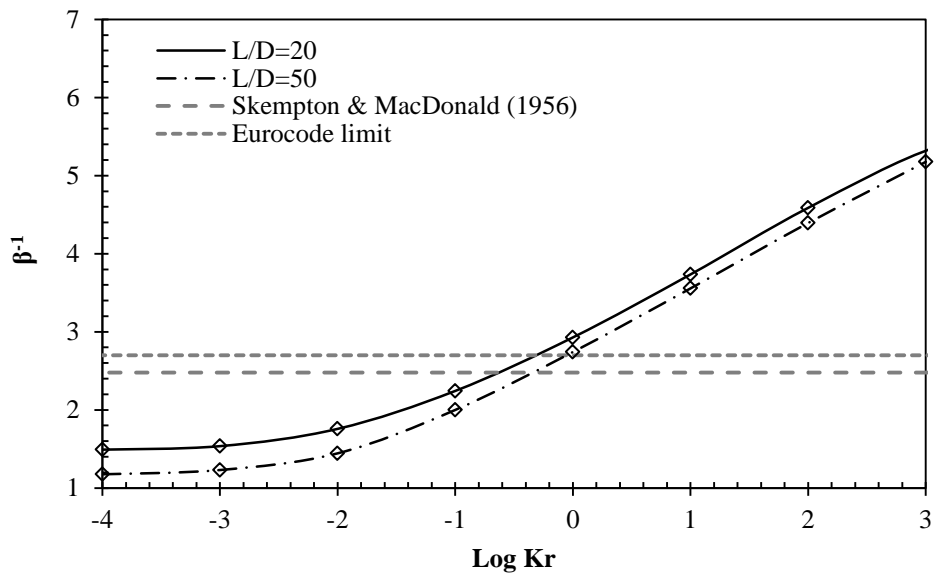


Fig. 19 Influence of L/D on β^{-1} ; $N=9$, $s/D=3$

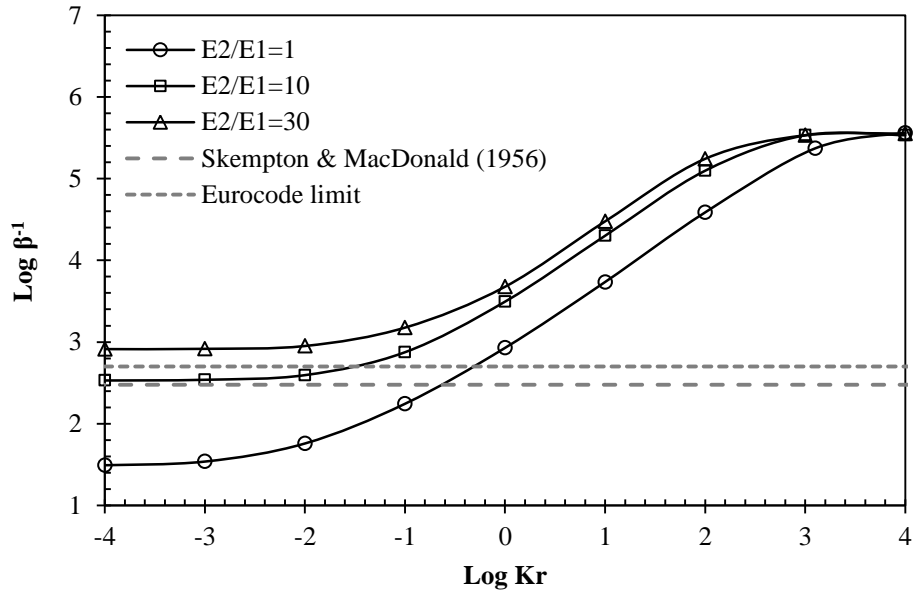


Fig. 20a Influence of E_2/E_1 on β^{-1} for $N=9$

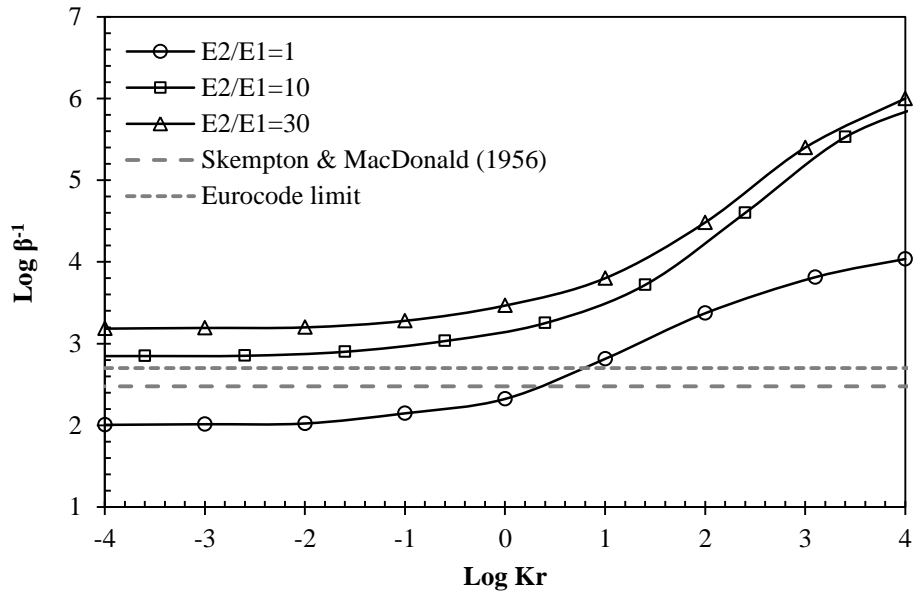


Fig. 20b Influence of E_2/E_1 on β^{-1} for $N=81$

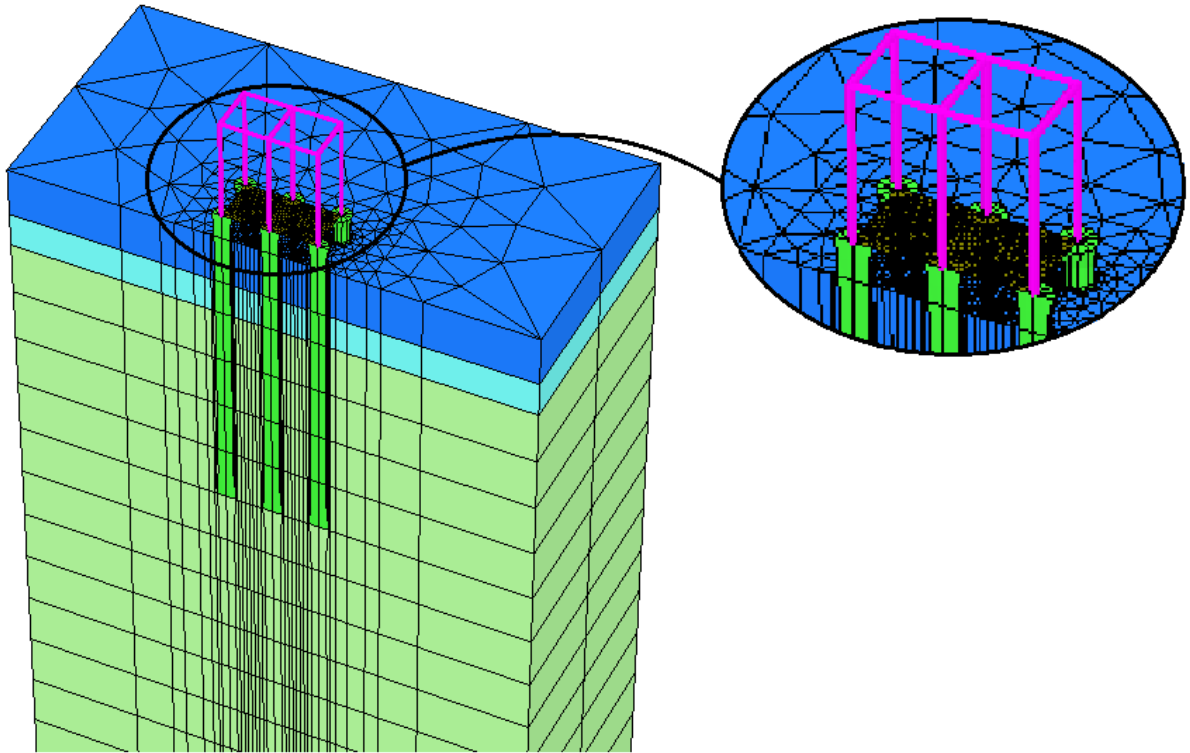


Fig. 21 Illustration of $n=1$ frame in FE model (half-symmetry) for $N=9$

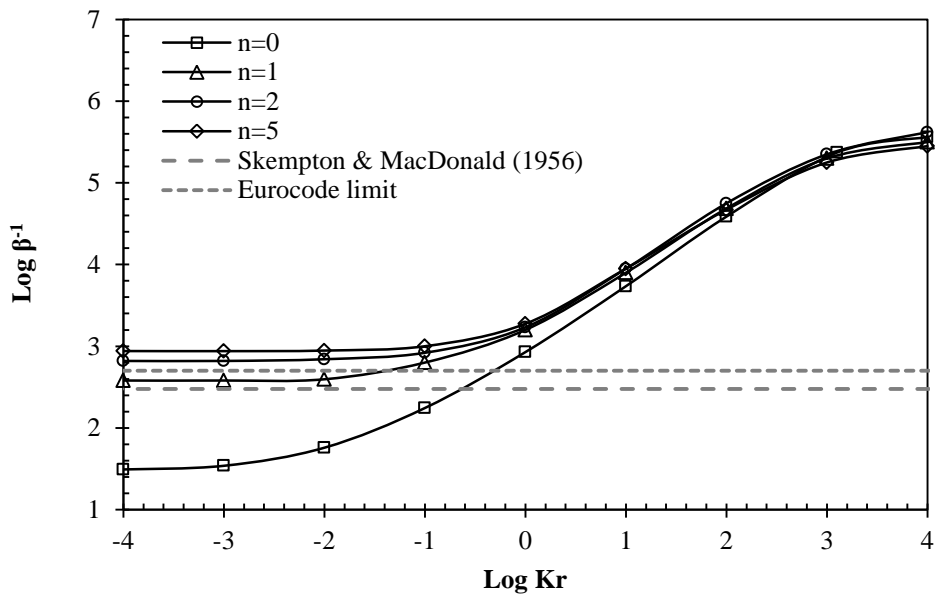


Fig. 22 Influence of supported structure on β^{-1} ; $N=9$

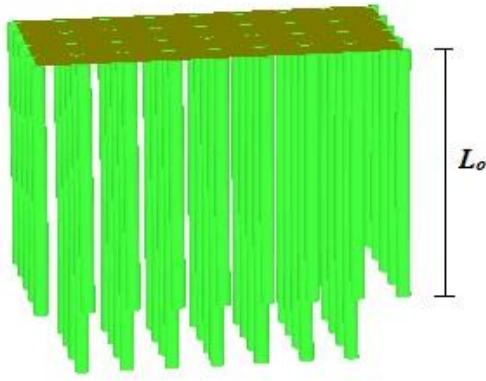


Fig. 23 Illustration of group with $L_o/L=0.75$

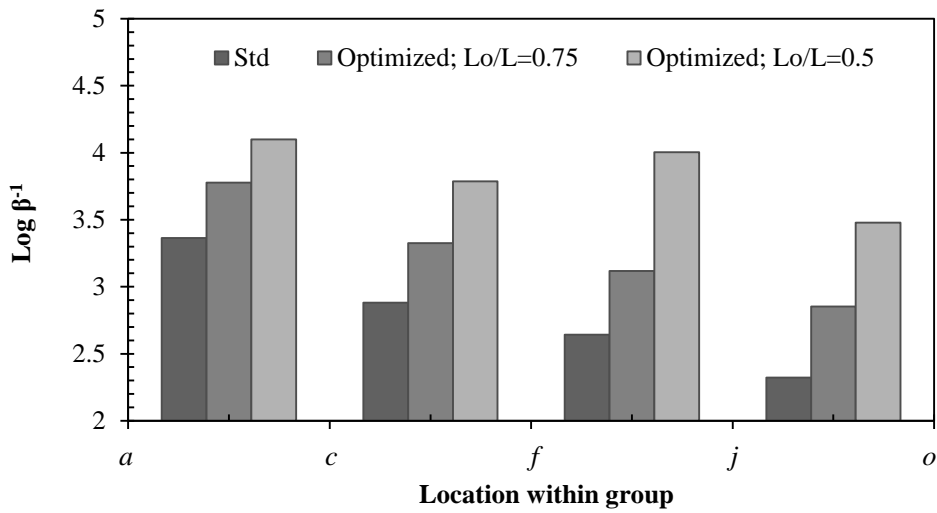


Fig. 24a Influence of L_o/L on β^{-1} distribution in optimized groups; $N=81$, $\log K_r=0$

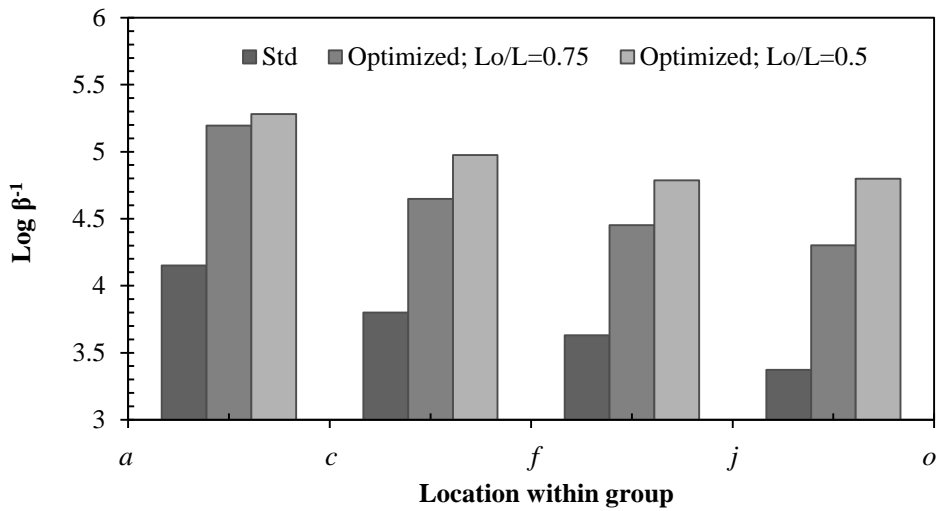
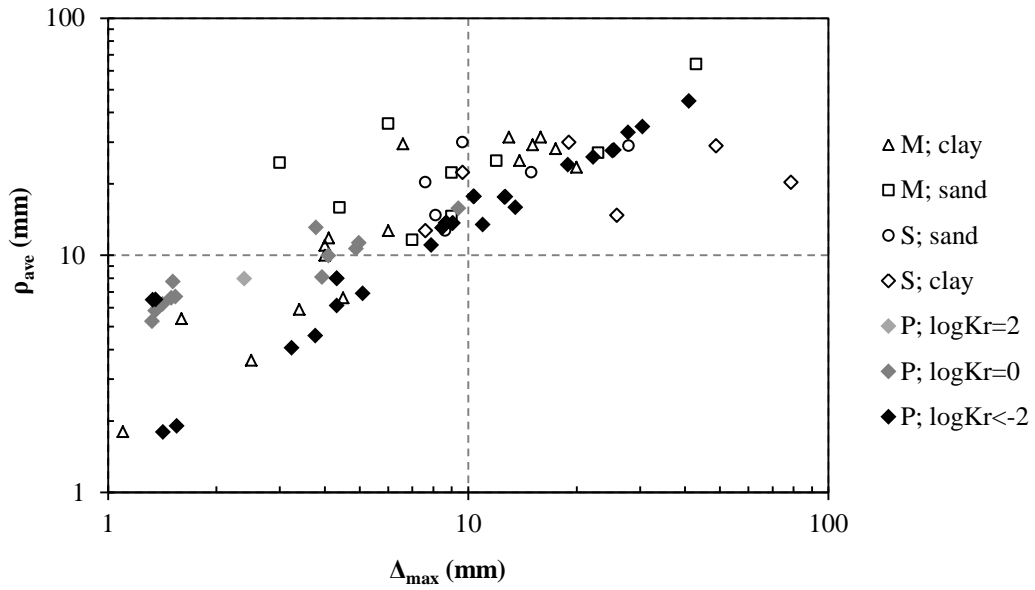
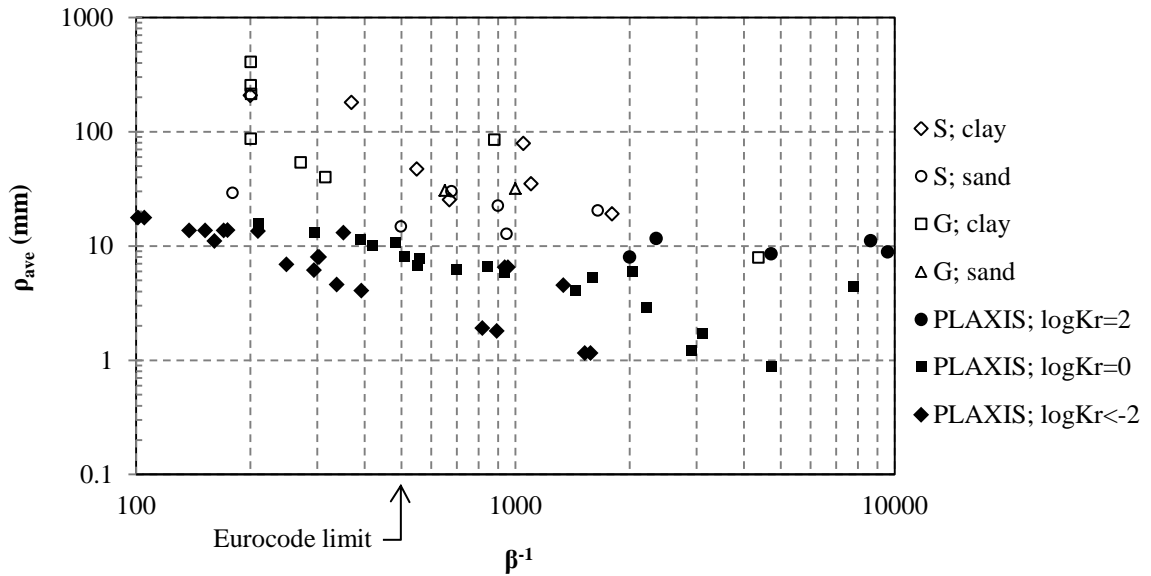


Fig. 24b Influence of L_o/L on β^{-1} distribution in optimized groups; $N=81$, $\log K_r=2$



M: Mandolini et al. (2005); S: Skempton and MacDonald (1956); P: PLAXIS results

Fig. 25 Comparison of numerical results with field data for ρ_{ave} Vs Δ_{max}



G: additional data documented by Grant et al. (1974)

Fig. 26 Comparison of numerical results with field data for ρ_{ave} Vs β^{-1}

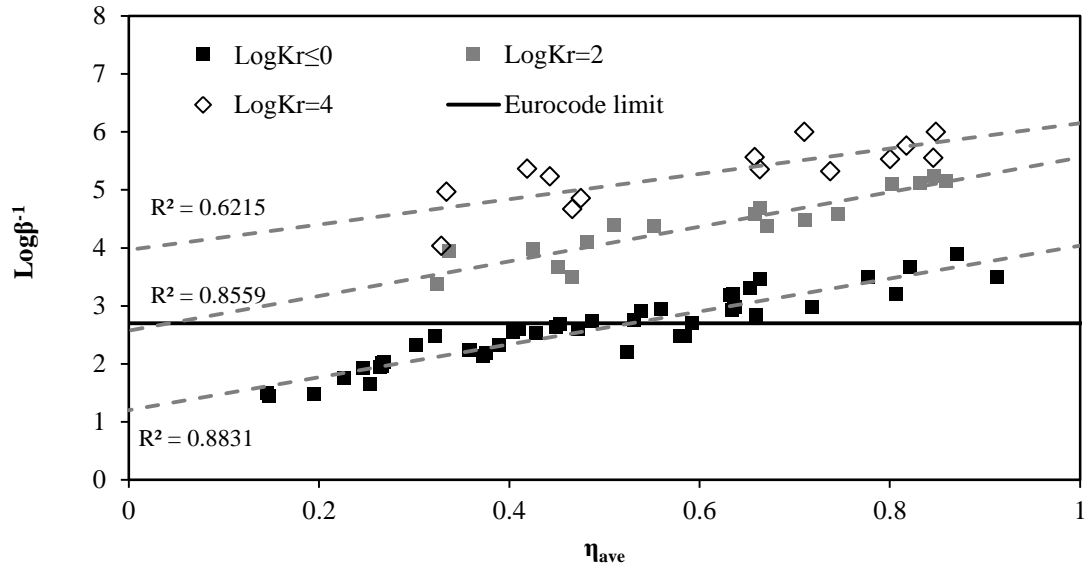


Fig. 27 Variation in β^{-1} with η_{ave} re-plotted